

# *Electrical measurements during fog in the United Arab Emirates*

Article

Accepted Version

Creative Commons: Attribution-Noncommercial-No Derivative Works 4.0

Alkamali, A. A., Ambaum, M. H.P. ORCID:  
<https://orcid.org/0000-0002-6824-8083> and Nicoll, K. A. ORCID: <https://orcid.org/0000-0001-5580-6325> (2024) Electrical measurements during fog in the United Arab Emirates. *Atmospheric Research*, 307. 107469. ISSN 1873-2895 doi: 10.1016/j.atmosres.2024.107469 Available at <https://centaur.reading.ac.uk/116651/>

It is advisable to refer to the publisher's version if you intend to cite from the work. See [Guidance on citing](#).

To link to this article DOI: <http://dx.doi.org/10.1016/j.atmosres.2024.107469>

Publisher: Elsevier

All outputs in CentAUR are protected by Intellectual Property Rights law, including copyright law. Copyright and IPR is retained by the creators or other copyright holders. Terms and conditions for use of this material are defined in the [End User Agreement](#).

[www.reading.ac.uk/centaur](http://www.reading.ac.uk/centaur)

**CentAUR**

Central Archive at the University of Reading  
Reading's research outputs online

## Electrical measurements during fog in the United Arab Emirates

Ahmad A. Alkamali<sup>12</sup>, Maarten H. P. Ambaum<sup>1</sup> & Keri A. Nicoll<sup>1</sup>

1. Department of Meteorology, University of Reading, United Kingdom
2. Department of Research and Weather Enhancement, National Center of Meteorology, United Arab Emirates

## Abstract

Distinct differences in electrical characteristics of the atmosphere are observed during clear and foggy laden air. The presence of droplets in the air causes the removal of natural cluster ions and hence, a change in the electrical properties, which is useful for fog detection, and potentially fog forecasting. In this study, we report on some of the first electrical measurements conducted during fog in the United Arab Emirates (UAE).

The analysis indicates that the Potential Gradient (PG) values observed during fog in the UAE were substantially higher than those previously reported in the literature (ranging from -1247 V/m to 1400 V/m). Furthermore, the PG during fog was often negative, with 93% of cases recording negative PG values (with median PG value of -397 V/m), particularly during wintertime fog events. A comparison with fog measurements conducted in the UK showed a stark contrast in PG behaviour between the two sites, with only positive PG values reported during fog in the UK (as is the case for the majority of PG fog studies reported in the literature), and higher PG variability in the UAE fogs. It is hypothesized that the unusual polarity of PG observed in UAE fog events may be attributed to the deposition of fog droplets, during which positive charges are transported from the top of the fog layer downwards toward the surface, thereby modifying PG. This deposition process is expected to be particularly active during the latter stages of the fog, when the droplet size distribution has fully evolved.

**Keywords:**

## Fog

## Potential Gradient

## Atmospheric Electricity

## 43 United Arab Emirates

44

## 1. Introduction

47 A continual electric field occurs in the atmosphere due to the presence of Earth's Global  
48 Atmospheric Electric Circuit (GEC). The GEC describes large scale current flow around the  
49 planet, caused by charge separation in thunderstorms, which generate a large potential difference  
50 between the conductive upper atmosphere and Earth's surface (Wilson, 1921). Measurements of  
51 atmospheric electricity can provide valuable information about the local meteorological conditions  
52 close to the observation site, including warning of disturbed weather, lightning, and fog formation  
53 (Nicoll, 2012). The most frequently observed surface quantity in atmospheric electricity is the  
54 vertical electric field, which is measured as the Potential Gradient<sup>1</sup> (PG) (Bennett and Harrison,  
55 2007).

57 The PG is closely related to local air conductivity, which originates from the presence of  
 58 atmospheric cluster ions. Natural ionisation, produced by galactic cosmic rays and Earth's  
 59 surface radioactivity, is the main cause of the finite electrical conductivity of air. Both positive and  
 60 negative air conductivities are strongly influenced by the presence of aerosol and water droplets  
 61 (Bennett and Harrison, 2008; Bennett and Harrison, 2009). Such aerosols include different particle  
 62 sizes, which can affect PG by reducing the mobility of the ions through attachment, particularly to  
 63 the larger particles (Yair and Yaniv, 2023), and consequently, removing the natural background  
 64 small ions. The reduction of ion number concentration results in a decrease in air conductivity. As  
 65 a result, the PG increases as the air conductivity decreases. The PG and air conductivity ( $\sigma$ ) are  
 66 related by Ohm's law:

$$J_z = \sigma PG \quad (1),$$

70 where  $J_z$  (which is assumed to remain constant) is the vertical conduction current density, which  
 71 flows as a result of the GEC (Rycroft et al., 2000).

74 Many studies have reported the marked difference in PG between fair<sup>2</sup> and disturbed weather  
75 (Dolezalek, 1973; Hoppel et al., 1986; Anisimov et al., 2005; Bennett and Harrison, 2009; Harrison  
76 and Nicoll, 2018). During fair weather conditions, the observed PG is normally positive with  
77 typical values ranging between 50 to 300 V/m depending on the site (Bennett and Harrison, 2007).  
78 In addition, the magnitude of PG variability during fair weather conditions is low when compared  
79 to that observed during disturbed weather conditions. However, the presence of aerosol  
80 concentrations in the air can cause substantial changes in PG (Bennett and Harrison, 2008).

<sup>1</sup>Potential Gradient (PG) is the difference in potential between the surface and a fixed point vertically above it, which is often used instead of the electric field (E) but with the opposite polarity (i.e.,  $PG = -E$ ) (Harrison and Nicoll, 2018).

2

<sup>2</sup>Fair-weather: For the conditions to be classified as “fair-weather”, the Met Office (in 1964) required four criteria, which are: (1) hours with no hydrometeors (i.e., no rain, hail, snow). (2) no low stratus clouds. (3) less than three eighths cumuliform clouds. (4) mean hourly wind speed less than 8 m/s (Harrison and Nicoll, 2018).

81 Fog occurs due to the condensation of water vapor to form droplets, which become suspended in  
82 air, leading to a reduction in visibility (typically defined as visibility less than 1 km). During fog,  
83 the PG is generally observed to increase substantially and become more variable. Harrison and  
84 Nicoll (2018) provided a good example of a foggy event observed in Reading, UK. A clear change  
85 in PG during the fog incident was reported, where the PG increased from about 150 V/m to 200 –  
86 250 V/m and became more variable. As the fog starts to dissipate, the PG decreased until it reached  
87 a steady value of 100 – 150 V/m, where the fog has completely dissipated.

88 A further comparison between foggy air and fair weather conditions was performed by Bennett  
89 and Harrison (2009). A clear difference was reported between the two conditions, where the  
90 measured PG was 400 V/m during fog while 100 V/m was observed during fair weather. The ratio  
91 of PG between foggy air and clear air can be obtained from Ohm's law assuming the fair weather  
92 current from the ionosphere to the surface is broadly constant across a fog event. This ratio of  
93 foggy air PG to clear air PG is only applicable with respect to the vertical conductivity, giving:  
94

$$96 \frac{PG(Fog)}{PG(Clear\ air)} = \frac{\sigma(Clear\ air)}{\sigma(Fog)} \quad (2),$$

97  
98 The presence of water drops and other aerosols leads to scavenging of free cluster ions that are  
99 responsible for the conductivity of the air (Harrison and Ambaum, 2008). As a consequence, foggy  
100 air exhibits lower conductivity compared to clear air.

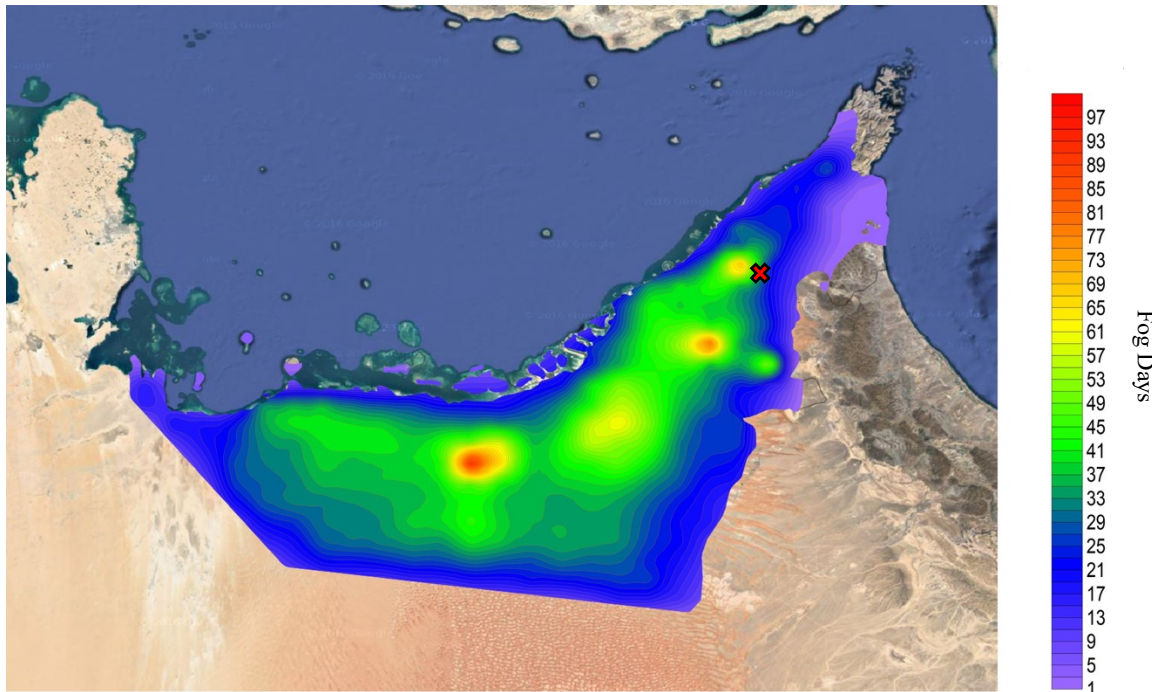
101  
102 Understanding the physics of fog has been a topic of significant interest due to its societal impact,  
103 particularly in terms of negative effects on transportation. Despite significant advances in  
104 numerical forecasting of fog during the past few decades, accurate fog prediction is still a challenge  
105 (e.g., Roman-Cascon et al., 2016). Previous research (Serbu and Trent, 1958; Dolezalek, 1973)  
106 has suggested that atmospheric electrical measurements may be useful for fog prediction, but this  
107 is still very much an open research question. Interest in the electrical properties of fog is also  
108 motivated by understanding the effect of charge on the behaviour of fog droplets (Harrison et al.,  
109 2022), with applications in fog dissipation (Tag, 1976; Zhang et al., 2023), and collection of fog  
110 droplets for water harvesting (Li et al., 2022).  
111

112  
113 This paper aims to characterise the electrical properties of fog in the United Arab Emirates (UAE)  
114 via a new dataset of atmospheric electrical observations. The measurement site is a desert location,  
115 where fog is prevalent during the winter months. Few papers in the literature report on fog  
116 observations from desert sites, so this is one of the first to characterise the electrical properties of  
117 fog in the desert. In this paper, Section 2 discusses the observation sites and instrumentation used.  
118 Section 3 reports observations of PG and meteorological parameters during several fog case  
119 studies, followed by a statistical analysis of all fog events captured in the UAE dataset. In order to  
120 compare the PG in fog in the UAE with those typically observed at mid latitude sites (which  
121 dominate the literature), Section 4 compares the UAE observations with those from a mid-latitude  
122 site in Reading, UK. The relationship between PG and visibility in the UAE and Reading is also  
123 considered in Section 4. Section 5 presents a discussion and Section 6 the conclusions.  
124

126      **2. Observation sites and instrumentation**

127  
128      The data presented in this paper is from a new observation site at Sanad Academy, Dubai, UAE  
129      ( $24^{\circ} 56' N$ ,  $55^{\circ} 30' E$ ), which was established in February 2021. The UAE (where the most  
130      prevailing aerosol type is composed of mineral dust (Nelli et al., 2021)) experiences frequent fog  
131      events throughout the year, with the highest frequency during the autumn and early winter months  
132      (de Villiers and van Heerden, 2007). This depends mainly on the sea-land breeze, which happens  
133      on over 70% of days during winter months in the UAE (Eager et al., 2008). The process starts with  
134      a transport of moisture from the sea during the day with the sea-breeze, which can extend up to  
135      200 km in land. During night time, the wind veers towards the land due to the temperature gradient  
136      caused by rapid cooling of air and hence, weakening the sea-breeze. A land breeze is common  
137      overnight in the UAE, which often lasts into the early morning and persists until the sea-breeze  
138      forms (Eager et al., 2008).

139  
140  
141      The most common fog type observed in the UAE is radiation fog (Weston et al., 2021), where the  
142      land cools rapidly at night and in turn causes the air above it to cool. As a result, water vapor  
143      condenses into liquid droplets and fog forms.



165      Figure 1. Annual number of fog days in the United Arab Emirates (UAE) for the year 2021. The  
166      location of the selected field site (Sanad Academy) is marked as red cross. This figure was obtained  
167      from the National Center of Meteorology (NCM), UAE, using data from NCM's automatic  
168      weather stations across the UAE, along with EUMETSAT infrared satellite images.

171 As the fog occurs, the horizontal visibility drops, which has historically led to significant economic  
172 losses in the UAE. These losses include transport disruptions such as air traffic delays, and car  
173 traffic accidents (Ali et al., 2013; Mohan et al., 2020). Figure 1 displays the number of fog days in  
174 the UAE during 2021, where most cases were observed in the internal regions of the country  
175 (ranging between 30 – 60 fog days) and some locations witnessed almost 100 fog days in 2021.  
176 This distribution of fog occurrences is typical for most years in the UAE. At Sanad Academy  
177 (marked as red cross in Figure 1), 27 fog days (both light and dense fog) were observed during  
178 2021. Dense fog cases were identified as cases when the visual range was  $\leq 1$  km for at least one  
179 hour period, while light cases (i.e., mist) were characterised by visibility ranges  $>1$  km and  $\leq 3$   
180 km. Additionally, a relative humidity (RH)  $>90\%$  was used as a supplementary indicator to  
181 distinguish fog from the presence of other aerosols.  
182

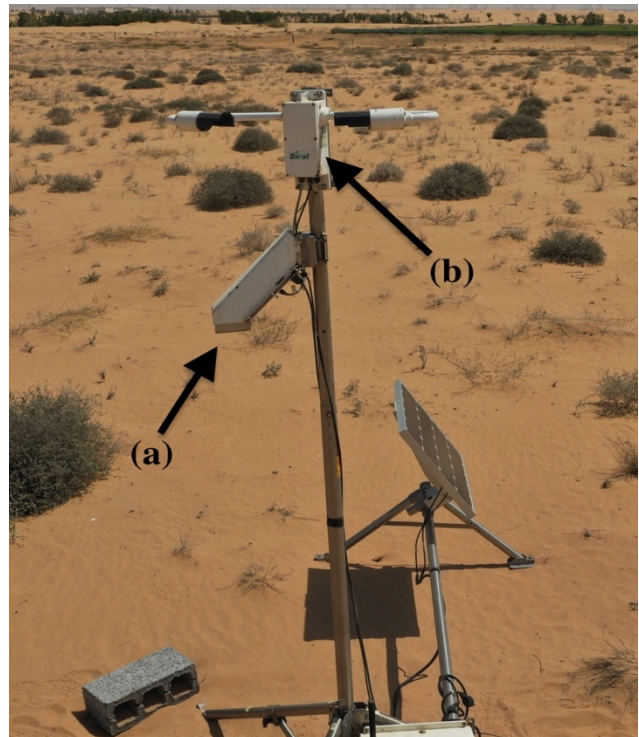
183 The measurement mast at Sanad Academy is located in the internal desert region of Dubai, which  
184 is a favorable location for radiation fog formation. As a result of radiative cooling, the air over the  
185 desert cools rapidly during the night, which causes the sea-breeze to weaken, leading to a reduction  
186 in the effects of warm maritime temperatures. As the surface radiative cooling intensifies, a surface  
187 inversion forms which traps the moisture near the surface and eventually, extends vertically until  
188 the dewpoint temperature is reached, where fog can form (Weston et al., 2021).  
189

190

(a)



(b)



191

Figure 2. The location of the observation site and instrumentation used. (a) Map of the UAE displaying the location of Sanad Academy, Dubai (obtained from Google Maps), and (b) sensors used to conduct this study, including (a) A downward facing electric field meter (Campbell CS110), used to measure the PG, and (b) The visibility sensor (Biral SWS-100).

192 Atmospheric electrical observations were conducted at Sanad Academy since February 2021 to  
193 present. Sanad Academy is an unmanned aircraft training facility in a desert location  
194 (approximately 45 km from the coastline), with the electrical instrumentation mast mounted on a  
195 sandy surface. The closest buildings to the instrumentation are 400 m away. **Figure 2 display the**  
196 **location of the field site along with the instrumentation used.** Instrumentation includes a Campbell  
197 CS110 electric field meter to measure the PG and Biral SWS-100 visibility sensor to measure the  
198 horizontal visibility. The CS110 was mounted at a height of 3 m above the ground, with a  
199 measurement range of  $\pm 20$  kV/m, at a sampling rate of 1-second. PG data were averaged, to 1-  
200 minute mean values to conduct the analysis described in this study. The visibility data were logged  
201 at 1-minute time resolution. Detailed explanation of the instrumentation used is given in Appendix  
202 A.

203 Meteorological data are also analysed in this paper, obtained from Al Marmoom Automatic  
204 Weather Station (AWS), Dubai ( $25^{\circ} 00' N, 55^{\circ} 30' E$ ). Meteorological observations include air  
205 temperature, RH, wind speed and direction, all logged at 15-minute time resolution. Al Marmoom  
206 is located approximately 9 km northeast of Sanad Academy (about 36 km from the coastline). The  
207 AWS used here is part of the National Center of Meteorology (NCM), Abu Dhabi, UAE. Due to  
208 the homogeneity of the terrain and the proximity, the weather conditions at Al Marmoom generally  
209 closely match those observed at the Sanad Academy field site.

210  
211 The observations in the UK were conducted at Reading University Atmospheric Observatory  
212 (RUAO), Reading ( $51.441^{\circ} N, 0.937^{\circ} W$ ). The observations were performed from December 2020  
213 to January 2021. At the site, a JCI131 electric field mill was used for PG measurements and a Biral  
214 visibility sensor to measure the visual range during the observation period. PG and visibility data  
215 were logged at 5-minute time resolution.

216  
217  
218  
219  
220  
221  
222

### 223 **3. Electrical characteristics of fog in the UAE**

224  
225 The following section presents two individual fog case studies from Sanad Academy, UAE,  
226 followed by a statistical analysis of all fog events from the Sanad Academy dataset. For an event  
227 to be classified as fog, the horizontal visibility must drop below 1 km as described in previous  
228 studies (Mohan et al., 2020; Tardif and Rasmussen, 2007; Weston et al., 2021) along with high  
229 RH which typically exceeds 90 %, this criterion is applied here to define fog events.

230  
231 Figure 3 presents data for the first fog case study on, March 31<sup>st</sup>, 2021, with PG and visibility  
232 (plotted on logarithmic scale) in Figure 3 (a), wind speed and direction in Figure 3 (b), and RH  
233 and temperature in Figure 3(c). During this day, several different types of meteorological  
234 conditions were observed at Sanad Academy which affected the PG, including early morning fog,  
235 an afternoon sea breeze front and a change in airmass in the evening, each of which is discussed  
236 in turn. Figure 3 (a) demonstrates high visibility ( $\geq 10$  km) and fair weather values of PG (~200

237 V/m) from 00-02 LT (UTC+4), in the period before fog forms. For comparison, the average typical  
238 diurnal variation in PG and visibility under fair weather conditions is displayed in Appendix A.2.  
239 As the condensation of haze droplets begins, the PG becomes negative, decreasing sharply down  
240 to -400 V/m at about 03 LT. This is followed by a steep decrease in visibility (down to 90 m)  
241 approximately an hour later (at 04 LT). Consequently, the dry bulb temperature was very low  
242 (about 16°C) and the RH was very high (reaching up to 100%), confirming the presence of a dense  
243 fog event. During the established fog period (04 – 07 LT) the PG is variable and mainly negative  
244 and fluctuates between 150 and -150 V/m. The existence of such negative PG values during fog is  
245 unusual, being rarely reported in the literature, and seem to defy theory, which predicts that a  
246 decrease in conductivity in fog should lead to an increase in PG (e.g., Harrison, 2012). This will  
247 be discussed further in Section 5.

248  
249 Following dissipation of the fog event around 07 LT, the afternoon of March 31<sup>st</sup> experienced a  
250 sea breeze, as shown in Figure 3. This is characterised by abrupt change in PG between 14 to 16  
251 LT, where the PG increased from 200 V/m up to 1000 V/m. During the same time, visibility  
252 decreased to 10 km, the wind speed increased from approximately 3 m/s to 6.5 m/s, and the wind  
253 veered from SE-SW and began blowing from W-NW (275° – 300°). These changes signify the  
254 arrival of the sea breeze front, which occurs due to temperature contrast between the land and the  
255 sea (Miller et al., 2003), a common phenomenon in the UAE (Eager et al., 2008). The large  
256 transient increase in PG during the sea breeze is characteristic of that reported in Nicoll et al.  
257 (2020) at another site (Al Ain international airport) located in the southeast of the UAE, and is  
258 thought to be associated with lofting of charged aerosols in the sea breeze front. During 2021, a  
259 total of 125 days of electrically active sea breeze cases were observed at Sanad Academy from a  
260 total of 238 days of data.

261  
262 In Figure 3 (a), the final distinct change in PG happened from about 21 – 00 LT, where a sudden  
263 decrease and polarity reversal in PG (from 200 V/m down to -200 V/m), occurs as well as an  
264 increase in the PG variability. Correspondingly, the visibility dropped from 10 km to 8 km. This  
265 sudden reduction in PG appears to be correlated with wind direction veering from NW to SE (300°  
266 to 135°), and also a decrease in wind speed from 6m/s to 1m/s. This shift in wind direction may  
267 indicate the change from a sea breeze to a weak land breeze, which would likely alter the aerosol  
268 properties over the measurement site. Sensitivity of the PG to wind direction was reported by  
269 Bennett and Harrison (2007), who found that variations in charged aerosol concentrations  
270 associated with wind direction changes, cause marked alterations in the PG. However, further  
271 analysis is still required to confirm the cause of the PG variations during this period.

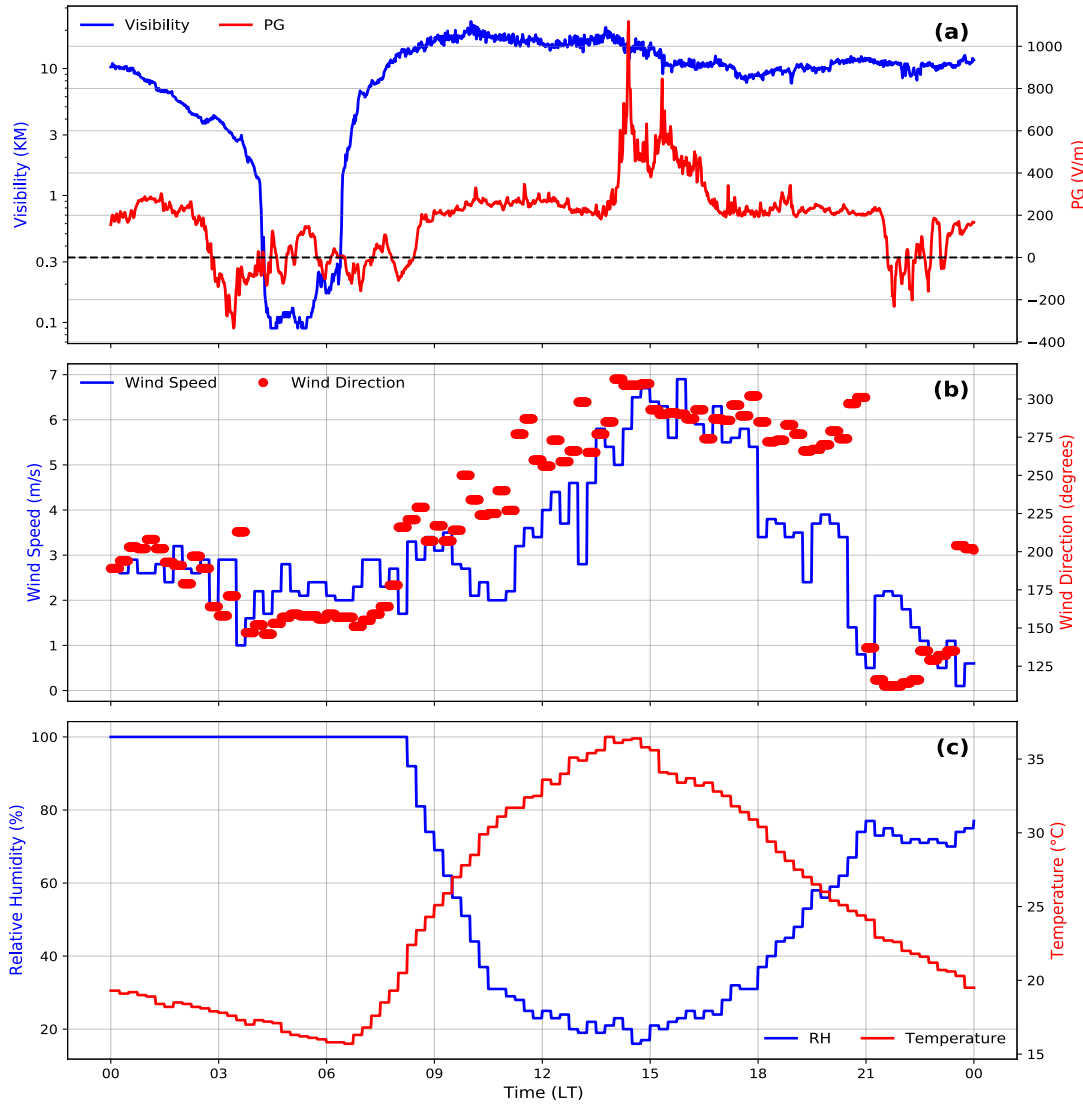
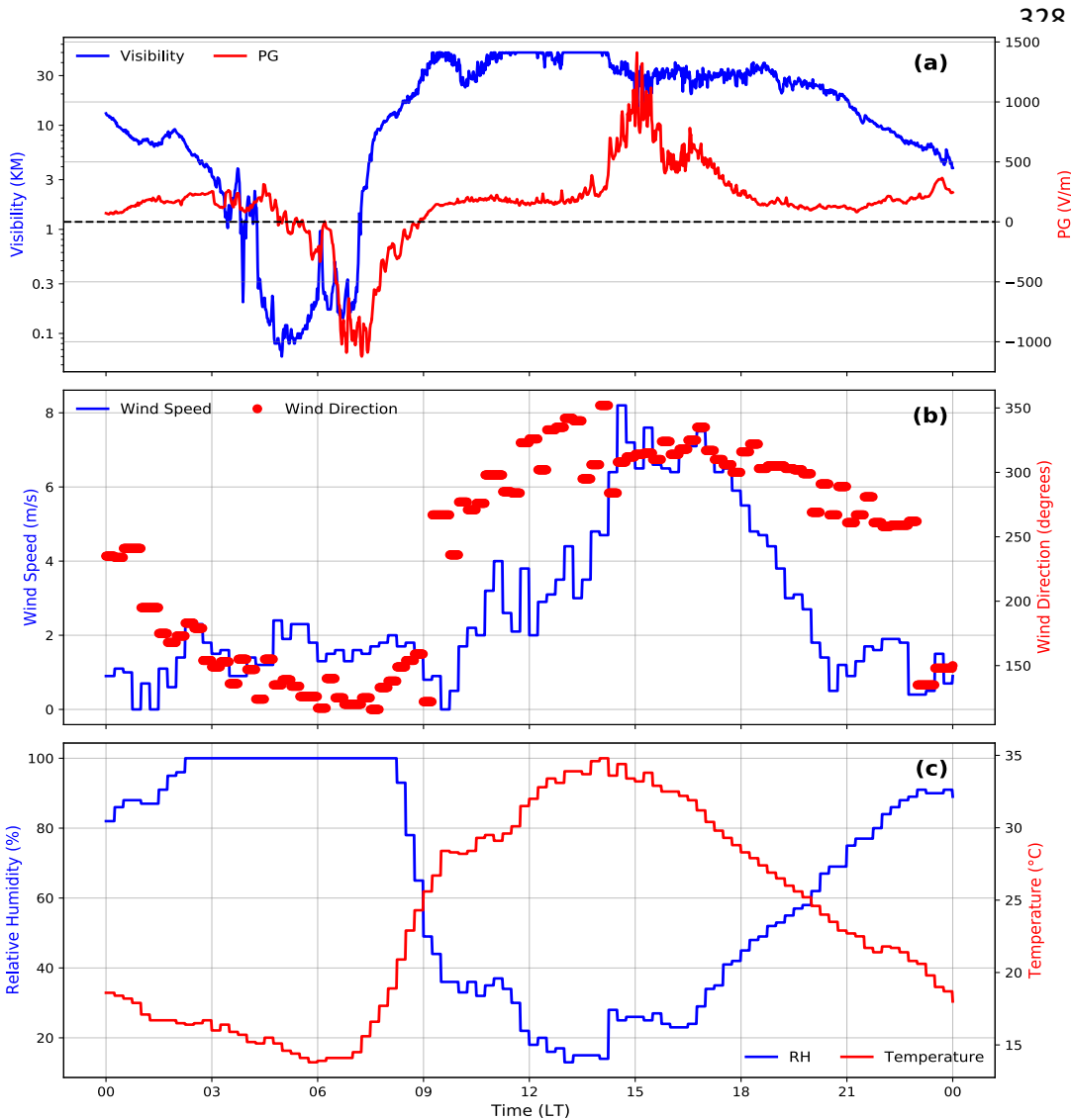


Figure 3. Diurnal variation in (a) PG and Visibility at Sanad Academy, (b) Wind speed and direction, and (c) Relative Humidity (RH) and Temperature from Al Marmoom AWS. The timeseries ranged from 00 UAE LT March 31st, 2021 till 00 UAE LT April 01st, 2021. PG and visibility are 1-minute time resolution while the wind speed and direction, RH and temperature are 15-minute time resolution. The wind direction was omitted for wind speeds of 0 m/s. The visibility data are presented on a logarithmic scale.

A second fog case study was observed on April 07<sup>th</sup>, 2021, presented in Figure 4. Similarly, as in the first case study presented in Figure 3, the fog event occurred during the early morning hours (04 – 07 LT) and was followed by a sea breeze event during the afternoon (14 – 18 LT). Figure 4 (a) shows a gradual decrease in visibility from 00 – 04 LT as haze starts to form, followed by a sharp decrease in visibility from 1 km to 60 m around 04 LT as the fog becomes more established. This fog case was further confirmed by the RH observation exceeding 95 % as seen in Figure 4 (c). The PG shows a small increase during the haze phase (from 100 – 300 V/m), but then decreases gradually from 04 LT as the fog forms. A sharp decrease to large negative values (-1100

318 V/m) is observed at 07 LT approximately 30 minutes before the fog dissipation (as indicated by  
 319 the increasing visibility at 08 LT, and a temperature rise from 14°C to 20°C). Although the  
 320 visibility has increased to non-fog values by 0830 LT the PG remains large and negative until 0900  
 321 LT. During the dissipation period, the fog droplets start to evaporate, but it takes some time for the  
 322 air to become entirely droplet free (and also any charge that existed on the fog droplets will remain  
 323 in the air). Thus, we expect it to take some time for the PG to return to its normal background value  
 324 after the fog dissipation stage. One of the distinctions between the two case studies is that the  
 325 largest change in PG in Figure 4 is approximately 1-2 hours following the fog formation (identified  
 326 from the reduction in visibility), whilst in Figure 3, the largest change in PG occurs at the start of  
 327 the fog event. The reasons for these discrepancies are still unclear.



360 Figure 4. Diurnal variation in (a) PG and Visibility at Sanad Academy, (b) Wind speed and  
 361 direction, and (c) Relative Humidity (RH) and Temperature from Al Marmoom AWS. The  
 362 timeseries is from 00 UAE LT April 07th, 2021 till 00 UAE LT April 08th, 2021. PG and visibility  
 363 are 1-minute time resolution while the wind speed and direction, RH and temperature are 15-

359

364 minute time resolution. The wind direction was omitted for wind speeds of 0 m/s. The visibility  
365 data are presented on a logarithmic scale.

366  
367 As in Figure 3, the arrival of an afternoon sea breeze front is evident in Figure 4, where the PG  
368 increases rapidly from 200 V/m to 1400 V/m between 14 – 17 LT. During this period, visibility  
369 reduces from 50 km down to 15 km and wind speed increases to 8 m/s, with a directional shift  
370 from SE to W-NW.

371  
372 Both case studies in Figures 3 and 4 demonstrate that the PG during fog conditions in the UAE is  
373 often large and negative, in contrast to most of the results reported in the literature (which are  
374 predominantly large and positive) (e.g., Serbu and Trent, 1958; Dolezalek, 1973; Yaniv and Yair,  
375 2023). To establish whether this type of PG behaviour is dominant during fog events in the UAE,  
376 statistical analysis of more fog events is required. From the Sanad Academy dataset, we have  
377 identified 27 fog events during 2021. 19 of these events were classified as dense fog (defined as  
378 cases when the visibility is  $\leq$  1 km with RH >90 %) and 8 classed as mist cases, where the visibility  
379 was greater than 1 km and less than or equal to 3 km and RH observations exceeding 90%. Only  
380 2 of the fog events occurred during the UAE summer months (June – August), with 25 events  
381 during winter/spring (February – April).

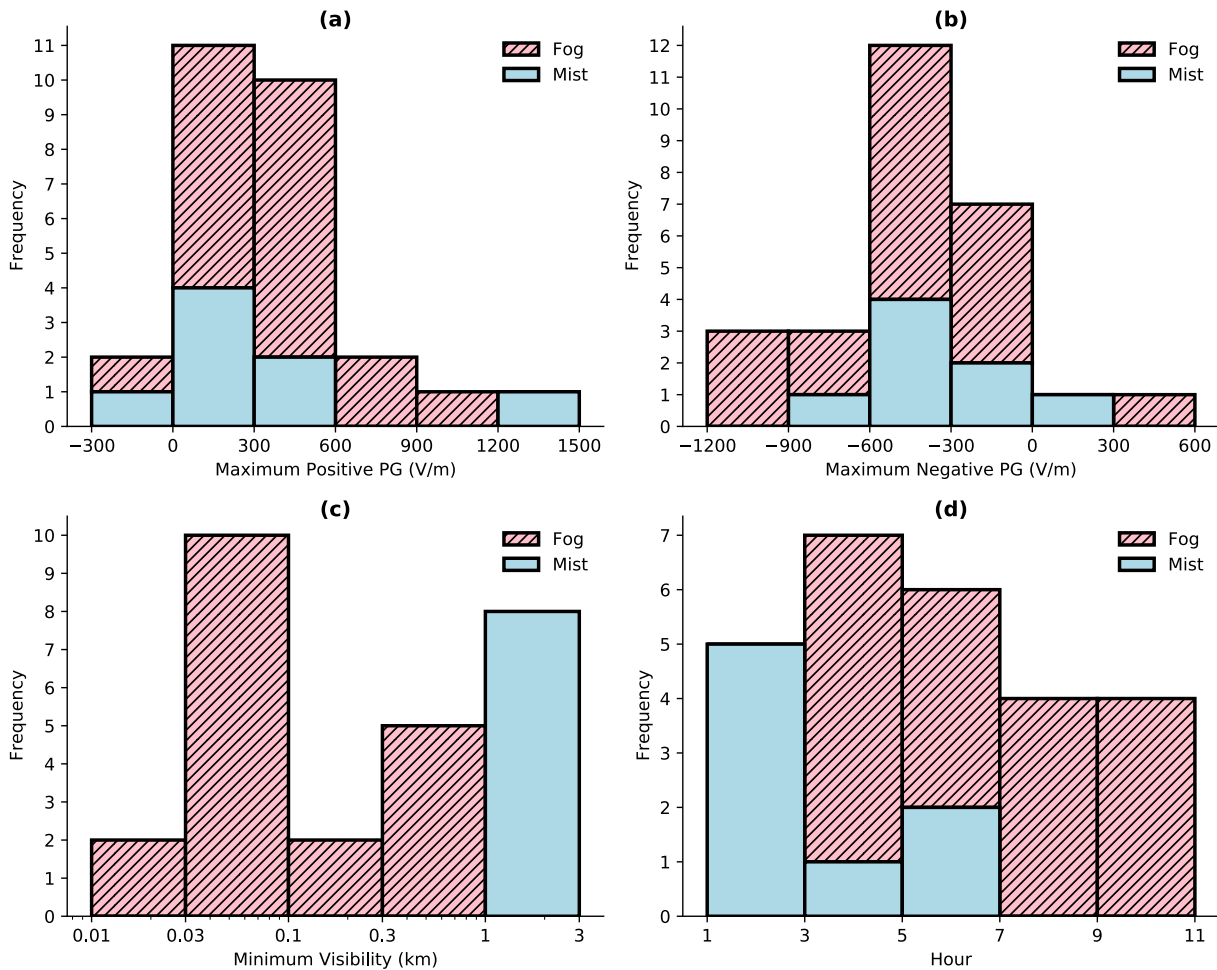
382  
383 Figure 5 displays the distribution of maximum positive PG, maximum negative PG, minimum  
384 visibility, and fog duration observed at Sanad Academy during all 27 fog events in 2021. Of the  
385 27 fog events, the largest maximum positive PG recorded was 1318 V/m (median = 311 V/m),  
386 which was observed during a summer fog event (both summer fog events exhibited only positive  
387 PG values, with values  $>$  1000 V/m in both events). This is large compared to most reported  
388 measurements of PG during fog in the literature (typically 300 – 800 V/m). Figure 5 (a) also  
389 demonstrates that in some of the fog events (2 events) the maximum PG is negative, and this occurs  
390 in both fog and mist cases.

391  
392 From Figure 5 (b), most PG values were clustered below 0 V/m (median = -397 V/m), with the  
393 lowest recorded negative PG value during fog events being -1247 V/m. This overall tendency  
394 towards negative PG was observed in 25 of the 27 fog events (93%), and predominantly during  
395 winter fog events. From the minimum visibility distribution in Figure 5 (c), it is apparent that  
396 approximately 70% of the fog events were classified as dense fog events, in which the lowest  
397 visibility recorded was 20 m (with median = 250 m). The winter fog events experienced lower  
398 visibilities in comparison to the summer fog events (with the minimum visibility in summer fog  
399 being 170 m).

400  
401 Figure 5 (d) shows the duration of the fog events, in which the median fog duration was 5 hours  
402 (comparable to other UAE fog events reported in the literature, such as Mohan et al., 2020), and  
403 the maximum duration observed was 10 hours. The two summer fog events exhibited much shorter  
404 durations, typically only lasting 1 hour.

405  
406  
407  
408

409  
410



411  
412  
413  
414  
415  
416

Figure 5. Stacked histograms of (a) maximum positive PG, (b) maximum negative PG, (c) minimum visibility, and (d) fog duration, during 19 dense fog events and 8 light fog events at Sanad Academy in 2021. Fog events were defined as instances when visibility was  $\leq 1$  km, while mist events were characterised by visibility  $> 1$  km and  $\leq 3$  km (with RH  $> 90\%$  in both conditions). Minimum visibility data are presented on a logarithmic scale.

417  
418  
419  
420  
421  
422  
423  
424

425           **4. Comparison of electrical characteristics of fog at different sites**

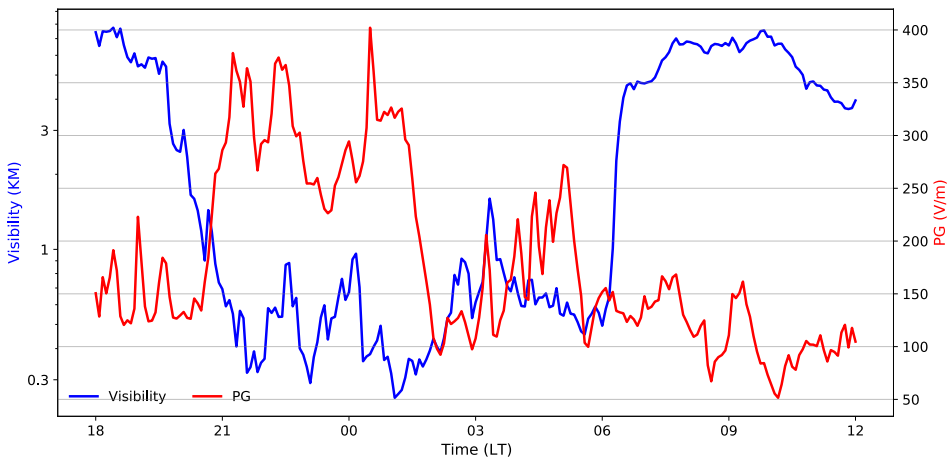
426

427           **4.1 United Kingdom case study**

428

429           In the preceding section, the electrical properties of fog in the UAE were investigated. In this  
430           section, a comparative analysis is undertaken to assess the electrical characteristics of fog in the  
431           UAE in relation to those observed at a typical midlatitude site, chosen to be Reading, UK.  
432           Generally, the UAE exhibits significantly higher aerosol loading in comparison to the UK, which  
433           has much more rainfall, more grass covered sites and, hence, lower aerosol loading (Nicoll et al.,  
434           2022). This discrepancy in background aerosol loading between the two countries potentially  
435           contributes to large differences in the observed electrical properties, which we seek to investigate.  
436           For this analysis, a fog case study from Reading is examined, followed by a comparison of  
437           statistical fog properties between the UAE and Reading sites for a small number of fog events. A  
438           timeseries of the meteorological and electrical parameters during a typical fog event at RUAO,  
439           UK is displayed in Figure 6 between December 31<sup>st</sup>, 2020 and January 01<sup>st</sup>, 2021.

440



453           Figure 6. Timeseries of PG and Visibility obtained at RUAO. The period used ranged from 18 UK  
454           LT December 31st, 2020 till 12 UK LT January 01st, 2021. The PG and visibility data were at 5-  
455           minute time resolution. The visibility data are presented on a logarithmic scale.

456

457           Figure 6 shows a sharp increase in PG from 120 to 400 V/m at 20:30 LT. At the same time, the  
458           visibility reduced rapidly from 7 km down to 250 m, signifying the presence of a dense fog event.  
459           The PG remains large and positive until 02 LT where it decreases (coinciding with an increase in  
460           visibility) but remains very variable. The small values of visibility (500 – 800 m) during the period  
461           from 02 – 06 LT indicate that fog is still present but is less dense than during the earlier part of the  
462           morning. After 06 LT, the visibility increases rapidly (from 700 m up to 5 km), and the PG returns  
463           to more fair weather values, indicating fog dissipation. The increase in PG during the fog formation  
464           stage shown here is typical of what is expected from the theory of a conductivity decrease in fog  
465           due to ion-aerosol attachment (e.g., Harrison, 2012), and reported by others in the literature (e.g.,

466 Anisimov et al., 2005; Bennett and Harrison, 2009). This contrasts with the negative PG values  
467 shown in UAE fogs in Section 3.

468  
469 To investigate the anomalous negative PG values observed in the UAE, it is useful to compare  
470 statistical information from UAE fog events with UK events. Table 1 shows a statistical summary  
471 of median PG, PG variability, maximum PG and minimum visibility during fog and non-fog  
472 (defined as visibility  $\geq 10$  km) for a continuous 10-day period in the UAE and UK. The timeframe  
473 selected for this analysis was from 21:00 to 09:00 LT in the UAE and from 18:00 to 09:00 LT in  
474 the UK, chosen to coincide with periods when fog is most likely to occur and to minimise the  
475 effects of other weather conditions. It should be noted that there are only 5 fog events (selected  
476 during the winter period) analysed for each site here. This small sample of fog events is not  
477 intended to give a full representation of fog characteristics for the two sites but is included here  
478 merely to provide an example of the general differences in PG behaviour between the two sites.  
479 The analyses for the fog events were computed only during periods where the visibility fell below  
480 1 km. In contrast, for the non-fog events, these quantities were calculated using visibility values  
481  $\geq 10$  km. The variability of PG is estimated as the interquartile range divided by 1.349 (i.e.,  
482 adjusted to be equivalent to the standard deviation for a normally distributed dataset).

483 Table 1 shows that in non-fog conditions the median PG is similar between the two sites (111 V/m  
484 in the UAE, and 104 V/m in the UK). This becomes very different in fog, with a negative median  
485 PG of -7 V/m in the UAE, but large and positive median PG of 235 V/m in the UK. The maximum  
486 PG values in the 5 fog cases are comparable for both sites (336 V/m in UAE and 402 V/m in UK),  
487 but, as is shown in Figure 5, in fog PG values can be much larger (up to 1400 V/m) in the UAE.  
488 Variability in PG was larger in the UAE for both non-fog (61 V/m compared to 26 V/m in UK)  
489 and fog cases (160 V/m compared to 102 V/m in UK) as would be expected from the increased  
490 aerosol loading in the UAE. The minimum visibility during the 5 UAE fog events was also found  
491 to be lower (40 m) than in the UK (250 m), signifying more dense fog events in the UAE.

492  
493

Region	Fog				Non-Fog				Number of Fog Cases
	Median PG (V/m)	PG Variability (V/m)	Max PG (V/m)	Min Visibility (km)	Median PG (V/m)	PG Variability (V/m)	Max PG (V/m)	Min Visibility (km)	
UAE	-7	160	336	0.04	111	61	460	10.02	5
UK	235	102	402	0.25	104	26	195	10.03	5

494  
495  
496  
497  
498  
499  
500  
501  
502  
503

Table 1. Summary of the statistical comparison performed during fog and non-fog conditions in  
the UAE (Sanad Academy) and the UK (RUAO). The observation period used for the UAE was  
from March 30<sup>th</sup>, 2021 till April 09<sup>th</sup>, 2021, while for the UK was from December 30<sup>th</sup>, 2020 till  
January 10<sup>th</sup>, 2021. The selected timings for the UAE were between 21 to 09 UAE LT only, while  
for the UK were between 18 to 09 UK LT only. Visibility range of  $\geq 10$  km was used for non-fog  
conditions. PG variability is expressed in terms of interquartile range (IQR) divided by 1.349.

504  
505  
506

## 507    4.2 PG and Visibility relationship

508  
509

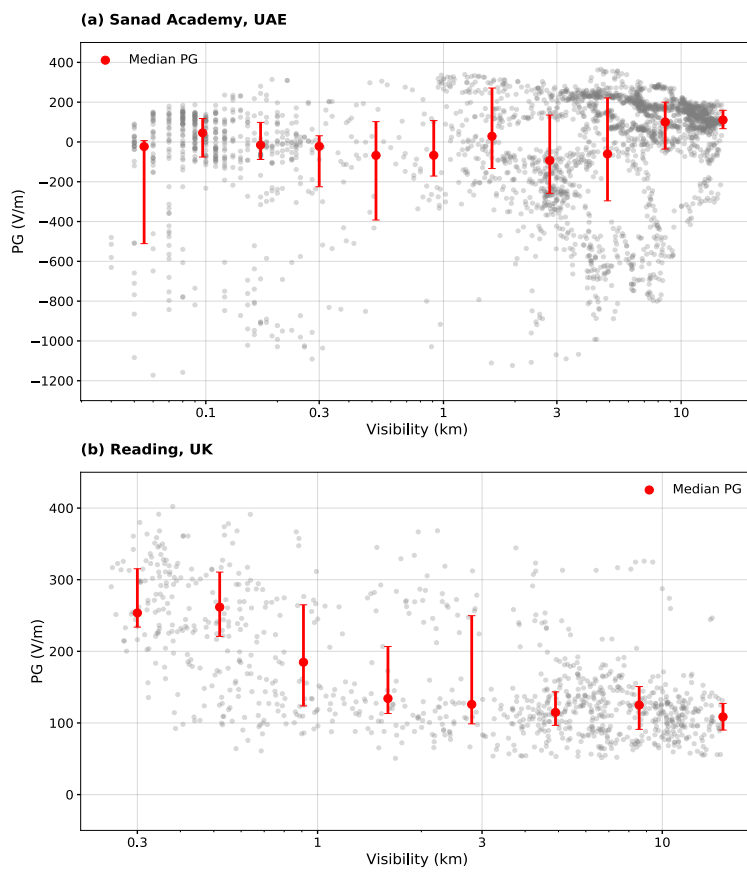
510 To investigate the anomalous negative PG values observed in the UAE further, it is instructive to  
511 examine the relationship between the PG and visibility for both the UAE and Reading sites during  
512 fog events, as illustrated in Figure 7. This analysis aims to test theoretical predictions, as reported  
513 by Harrison (2012), which suggest a predictable relationship between the PG and the visibility due  
514 to the close association between PG and air conductivity. Figure 7 shows PG and visibility data  
515 for the 5 fog events in Table 1, for (a) the UAE (Sanad Academy), and (b) Reading, UK. In fog  
516 events observed in the UK (Figure 7 (b)), a clear relationship is demonstrated between the PG and  
517 the visibility. PG is largest for the lowest visibility values and decreases towards more fair weather  
518 values as the visibility increases. At higher visibilities ( $> 1$  km), the PG ceases to change with  
519 increasing visibility and instead becomes steady, reaching an asymptotic behaviour. These findings  
520 align with the previous observations of PG behaviour during fog in the UK, as reported in Harrison  
521 (2012) and Harrison and Nicoll (2018).

522  
523

524 Conversely, the relationship observed between PG and visibility during fog events in the UAE  
525 (Figure 7 (a)) is much less obvious, with no clear relationship observed between the two. Also, as  
526 noted previously, many of the PG values are negative. These findings suggest that the PG changes  
527 observed during many fog events in the UAE are not dominated by conductivity changes (which  
528 are indicative of visibility variations). **It is possible that charging of the fog droplets (which is**  
529 **discussed more fully in section 5, and not included in the theoretical relationship derived in**  
530 **Harrison (2012)) modifies the PG/visibility relationship beyond what is expected from the neutral**  
531 **fog droplet case, but further measurements are needed to confirm this.**

532

533  
534  
535  
536  
537  
538  
539  
540  
541  
542  
543  
544  
545  
546  
547  
548  
549  
550  
551  
552  
553  
554  
555  
556  
557



558 Figure 7. Relationship between PG and visibility during fog at (a) Sanad Academy and (b) Reading  
559 University Atmospheric Observatory (RUAO). Red dot represents the median PG values including  
560 interquartile ranges binned based on visibility at Sanad Academy (11 bins from 0.055 to 15 km)  
561 and RUAO (8 bins from 0.30 to 15 km). Data from Sanad Academy was from March 30th, 2021  
562 to April 09th, 2021 with time selected between 21 to 09 UAE LT only, while for RUAO data was  
563 from December 30th, 2020 till January 10th, 2021 with time selected between 18 to 09 UK LT  
564 only. During the selected periods, 5 fog cases were observed at each site. The visibility data are  
565 presented on a logarithmic scale.

566  
567

## 5. Discussion

568  
569  
570  
571  
572  
573  
574  
575  
576  
577

Based on the analysis presented in this study, it is evident that the electrical characteristics of fog in the UAE differ from those typically observed at some midlatitude sites such as the UK. The observed transition of the PG behaviour to negative values during the fog events in the UAE contradicts the findings of many previous studies (e.g., Nizamuddin and Ramanadham, 1983; Anisimov et al., 2005; Bennett and Harrison, 2007; Bennett and Harrison, 2008; Harrison, 2012; Harrison and Nicoll, 2018; Yair and Yaniv, 2023). These studies have reported an increase in the PG, which is likely attributed to the removal of ions by fog droplets, resulting in a decrease in air conductivity, through Ohm's law (equation 1). Figure 4 demonstrate that in fog events at Sanad, the PG increases as expected during the initial fog formation stage, but then decreases and becomes

578 negative. In order for the PG to become negative during fog it is likely that an additional charge  
579 separation/generation mechanism (either natural or artificially) must be present. Previous research  
580 by Chalmers and Little (1947) and Chalmers (1952) measured negative PG values during fog,  
581 which they attributed to generation of negatively charged ions from power cables. This negative  
582 charge is likely to be transferred to the fog droplets, potentially leading to a reversal in polarity of  
583 the PG. Although the measurement mast at Sanad Academy is approximately 400 m from any  
584 buildings, with no known sources of artificial charge generation, it is possible (though unlikely)  
585 that nearby factories or construction work could be responsible for the negative PG values.  
586

587 Another possible explanation is related to the observation that fogs at Sanad Academy are  
588 noticeably wet, which we refer to here as “drizzling fog”. Often the desert surface during such fog  
589 events is extremely damp, with visible droplets on equipment. Evidence of large fog droplet  
590 diameters observed in the UAE is discussed in the findings of Weston et al. (2021), where the peak  
591 of the droplet size distribution has been measured to be 25  $\mu\text{m}$  during fog in the UAE, compared  
592 to peaks below 10  $\mu\text{m}$  in some midlatitude sites. It is possible that very large “drizzling” fog  
593 droplets may splash and release charged ions on impact with the surface (and the surface of the  
594 field mill), potentially leading to negative values of PG, as is observed during rain events (e.g.,  
595 Simpson, 1909; Levin and Hobs, 1971; Kamra et al., 2015), but the rain rates required for splashing  
596 to occur are likely to be larger than would occur during “drizzling fog” conditions.  
597

598 An alternative, more likely, hypothesis is related to the deposition of droplets, which is a common  
599 phenomenon during radiation fog (Duynkerke, 1991). In theory, within a stable cloud layer,  
600 positive charges are likely to accumulate on droplets at the cloud top due to the vertical current  
601 from the global electric circuit as it flows through the vertical conductivity gradient at the boundary  
602 between the clear air and droplet-laden air (Harrison et al., 2020; Nicoll and Harrison 2010; Zhou  
603 and Tinsley 2012). We hypothesize that the conductivity change at the upper boundary of a fog  
604 layer is similar to that in a stratiform layer, and is likely to produce positive charge as suggested  
605 by theory. Although the authors are not aware of any charge measurements of this phenomena in  
606 fog, it is well documented in the stratiform cloud case (Nicoll and Harrison, 2016), where it has  
607 been observed that the charge at the cloud top is often larger than at cloud base, due to strong  
608 temperature inversions at cloud top, which provide a “sharper” transition between clear and cloudy  
609 air. Vertical profiles of microphysical fog droplet properties by Egli et al., (2015) demonstrate  
610 that fog tops are often associated with strong temperature inversions, and sharp changes in fog  
611 droplet concentrations (as is the case for stratiform clouds), therefore it is reasonable to suggest  
612 that fog tops will be similarly charged to stratiform clouds. Once the droplets become large  
613 enough, deposition of the fog droplets will transport the positive charge (which exists on the  
614 droplets) downwards towards the surface, which is likely to modify the PG, causing it to decrease  
615 and potentially become negative. This is expected to occur particularly during the latter stages of  
616 fog events where the droplet size distribution has fully evolved (Katata 2014; Lovett 1984). The  
617 formation of larger drops and their subsequent deposition is a characteristic of the dissolving of  
618 long-lived fog.  
619

620 The observation that the negative PG values only occur during winter fogs (when the fogs are  
621 denser and long lived), supports the possibility that these fogs have the potential to contain larger  
622 droplets than fogs during the summer months, and also that the conductivity gradient between clear

623 and foggy air at fog top is larger (which, theoretically, leads to more positive charge), but more  
624 research is required to fully explain the occurrence of negative PG values during fog in the UAE.  
625

626 The large positive values of PG observed in the UAE summer months (up to 1400 V/m) are  
627 generally larger than those reported in the literature (Nizamuddin and Ramanadham, 1983;  
628 Anisimov et al., 2005; Bennett and Harrison, 2007; Bennett and Harrison, 2009; Harrison and  
629 Nicoll, 2018; Yair and Yaniv, 2023), which may be related to differences in the fog droplet number  
630 concentration and size distributions between the various sites. The high aerosol content in the UAE  
631 (from lofted sand and industrial pollution) may also influence the fog droplet properties, as well  
632 as the background conductivity, which has likely implications for the PG (e.g., Zheng, 2013; Nicoll  
633 et al., 2020), which also needs further investigation.

## 638 6. Conclusions

639 Forecasting fog onset and dissipation remains a challenging task despite the improvements in  
640 numerical weather prediction (NWP) models. The need of improving the forecast accuracy is  
641 required to mitigate major losses caused by fog. This study aims to investigate whether electrical  
642 properties of the atmosphere may serve as a useful tool to aid fog forecasting, by understanding  
643 the electrical characteristics of fog in the UAE, which experiences regular fog events. These  
644 surface electrical measurements of fog are the first to be conducted in the UAE, and hence, are  
645 compared to previous studies made in the UK.

646 This study established that the electrical behavior of fog in the UAE is different to that in the UK,  
647 especially during winter fog. Unlike in previous studies (Nizamuddin and Ramanadham, 1983;  
648 Anisimov et al., 2005; Bennett and Harrison, 2007; Bennett and Harrison, 2008; Harrison, 2012;  
649 Harrison and Nicoll, 2018; Yair and Yaniv, 2023), the PG in the UAE experienced opposite  
650 polarity during the presence of fog. 93% (25 out of 27) of fog cases included periods of negative  
651 PG, with the median minimum PG during fog being -397 V/m. Analysis of the relationship  
652 between PG and visibility in the UAE during fog conditions showed no clear correlation between  
653 the two, suggesting that PG changes in fog in the UAE are not dominated by conductivity changes.

654 The transition of PG to negative values during fog is considered an unusual phenomenon, which  
655 we hypothesize to occur due to the deposition of positively charged fog droplets. The positive  
656 charge is hypothesized to exist at the top of the fog layer, from vertical current flow in the Global  
657 Electric Circuit. During the deposition process, positive charge is suggested to be transported  
658 downwards toward the surface, modifying the surface PG. This is likely to be particularly active  
659 during the latter stages of the fog when the droplet size distribution has fully evolved. The negative  
660 PG did not occur during summer time fog events, where the PG was observed to increase solely  
661 as a result of the formation of fog over a brief duration. Hence, the droplets do not have enough  
662 time to grow in size. Currently, our research focuses on analysing droplet size distribution using  
663 an optical sensor to investigate the growth of droplet size during fog events in the UAE to  
664 investigate this hypothesis further.

669 Furthermore, the quantified variability of the PG during foggy and non-foggy conditions were used  
670 to compare between the UAE and the UK. The results showed that the PG exhibited significantly  
671 higher variability in the UAE during foggy conditions, with a measured variability of 160 V/m  
672 compared to 102 V/m in the UK. In addition, the median PG during fog in the UAE was very  
673 different from that observed in the UK, with median of -7 V/m compared to 235 V/m in the UK.  
674 This may occur due to differences in turbulent characteristics of the fog, differences in droplet  
675 size/number/ charge properties, or variations in the fog droplet charge between the two  
676 environments.

677

678 It can be concluded that fog occurrences during the winter season in the UAE consistently exhibit  
679 different PG behaviour to those generally reported in the literature, making it an unusual  
680 phenomenon that diverges from fog events observed in clean air environments.

681

682

683

684

685

## 686 **Acknowledgments**

687

688 AAK acknowledges a studentship from the Scholarship Coordination Office (SCO)  
689 Presidential Court, Abu Dhabi, UAE. The National Center of Meteorology (NCM) are  
690 also acknowledged for sharing Al Marmoom AWS and satellite images. Our thanks also  
691 go to Samer Akoum who helped with our field setup. We would also like to thank Sanad  
692 Academy team for allowing us to use their site.

693

694

## 695 **Data Availability**

696

697 Potential gradient and visibility data are openly available and can be accessed online  
698 from the University of Reading Data Repository at <https://doi.org/10.17864/1947.000501>.  
699 Wind speed, wind direction, and EUMETSAT satellite data can be requested from the  
700 National Center of Meteorology, UAE.

701

702

703

704

705

706

707

708

709

710

711

712  
713      **References**  
714

715      Agarwal, A., Bhattacharya, S., Chaudhari, S., 2020. Electric Field Mill, an Effective  
716      Methodology to Measure the Localized Lower Atmospheric Electric Field. *Mat. Proc.* 29.  
717      440 – 447. DOI: 10.1016/j.matpr.2020.07.297.

718      Ali, O.W.B., Al-Harthei, H., Garib, A., 2013. Real-Time Fog Warning System for the Abu  
719      Dhabi Emirate (UAE). *J. Traff. Log. Eng.* 1. 213 – 217. DOI: 10.12720/jtle.1.2.213-217.

720      Anisimov, S.V., Mareev, E.A., Shikhova, N.M., Sorokin, A.E., Dmitriev, E.M., 2005. On the  
721      electro-dynamical characteristics of fog. *J. Atmos. Res.* 76. 16 – 28. DOI:  
722      10.1016/j.atmosres.2004.11.026.

723      Bateman, M.G., Stewart, M.F., Podgorny, S.J., Christian, H.J., Mach, D.M., Blakeslee, R.J.,  
724      Bailey, J.C., Daskar, D., 2007. A Low-Noise, Microprocessor- Controlled, Internally  
725      Digitizing Rotating-Vane Electric Field Mill for Airborne Platforms. *Amer. Meteor. Soc.* 24.  
726      1245 – 1255. DOI: 10.1175/JTECH2039.1.

727      Bennett, A.J., Harrison, R.G., 2007. Atmospheric electricity in different weather conditions.  
728      *Roy. Meteor. Soc.* 62. 277 – 283. DOI: 10.1002/wea.97.

729      Bennett, A.J., Harrison, R.G., 2008. Variability in surface atmospheric electric field  
730      measurements. *J. Phys.: Conf. Ser.* 142. DOI: 10.1088/1742-6596/142/1/012046.

731      Bennett, A.J., Harrison, R.G., 2009. Evidence for global circuit current flow through water  
732      droplet layer. *J. Atmos. Solar-Terr. Phys.* 71. 1219 – 1221. DOI: 10.1016/j.jastp.2009.04.011.

733      Chalmers, J.A., Little, E.W.R., 1947. Currents of atmospheric electricity. *Terr. Magn. Atmos.*  
734      *Electr.* 52. 239 – 260. DOI: 10.1029/TE052i002p00239.

735      Chalmers, J.A., 1952. Negative electric fields in mist and fog. *J. Atmos. Terr. Phys.* 2. 155 –  
736      159. DOI: 10.1016/0021-9169(52)90060-3.

737      De Villiers, M.P., van Heerden, J., 2007. Fog at Abu Dhabi International Airport. *Roy. Meteor.*  
738      *Soc.* 62. 209 – 214. DOI: 10.1002/wea.45.

739      Dolezalek, H., 1973. On the Electro-atmospheric Fog Effect. *Pure Applied Geophys.* 105. 907  
740      – 909. DOI: 10.1007/BF00875840.

741      Duynkerke, P.G., 1991: Radiation Fog: A Comparison of Model Simulation with Detailed  
742      Observations. *Mon. Wea. Rev.* 119. 324 – 341. DOI: 10.1175/1520-  
743      0493(1991)119<0324:RFACOM>2.0.CO;2.

744      Eager, E.R., Raman, S., Wootten, A., Westphal, D.L., Reid, J.S., Al Mandoos, A., 2008. A  
745      climatological study of the sea and land breezes in the Arabian Gulf region. *J. Geophys. Res.*  
746      113. 1 – 12. DOI: 10.1029/2007JD009710.

747  
748  
749  
750  
751  
752  
753  
754  
755

756 Egli, S., Maier, F., Bendix, J., Thies, B., 2015. Vertical distribution of microphysical properties  
757 in radiation fogs – A case study. *J. Atmos. Res.* 151. 130 – 145. DOI:  
758 10.1016/j.atmosres.2014.05.027.

759

760 Harrison, R.G., 2012. Aerosol-induced correlation between visibility and atmospheric  
761 electricity. *J. Aero. Sci.* 52. 121 – 126. DOI: 10.1016/j.jaerosci.2012.04.011.

762

763 Harrison, R.G., 2011. Fair weather atmospheric electricity. *J. Phys.: Conf. Ser.* 301.  
764 DOI:10.1088/1742-6596/301/1/012001.

765

766 Harrison, R.G., Marlton, G.J., Ambaum, M.H.P., Nicoll, K.A., 2022. Modifying natural  
767 droplet systems by charge injection. *Phys. Rev. Res.* 4. 1 – 6. DOI:  
768 10.1103/PhysRevResearch.4.L022050.

769

770 Harrison, R.G., Nicoll, K.A., 2018. Fair weather criteria for atmospheric electricity  
771 measurements. *J. Atmos. Solar-Terr. Phys.* 179. 239 – 250. DOI:  
772 10.1016/j.jastp.2018.07.008.

773

774 Harrison, R.G., Ambaum, M.H.P., 2008. Enhancement of cloud formation by droplet  
775 charging. *Proc. Roy. Soc.* 464. 2561 – 2573. DOI: 10.1098/rspa.2008.0009.

776

777 Harrison, R.G., Nicoll, K.A., Mareev, E., Slyunyaev, N., Rycroft, M.J., 2020. Extensive layer  
778 clouds in the global electric circuit: their effects on vertical charge distribution and storage.  
779 *Proc. Roy. Soc.* 476. 1471 – 2946. DOI: 10.1098/rspa. 2019.0758.

780

781 Harrison, R.G., 2015. Meteorological Measurements and Instrumentation. John Wiley & Sons,  
782 Ltd. 257 pp.

783

784 Hoppel, W.A., Anderson, R.V., Willett, J.C., 1986. Atmospheric Electricity in the Planetary  
785 Boundary Layer, The Earth's Electrical Environment. National Academy Press. 149 – 165.

786

787 Izett, J.G., van de Wiel, B.J.H., Baas, P., Bosveld, F.C., 2018. Understanding and Reducing  
788 False Alarms in Observational Fog Prediction. *Boundary-Lay. Meteor.* 169. 347 – 372. DOI:  
789 10.1007/s10546-018-0374-2.

790

791 Kamra, A.K., Gautam, A.S., Siingh, D., 2015. Charged nanoparticles produced by splashing  
792 of raindrops. *J. Geophy. Res.* 120. 6669 – 6681. DOI: 10.1002/2015JD023320.

793

794 Katata, G., 2014. Fogwater deposition modeling for terrestrial ecosystem: A review of  
795 developments and measurements. *J. Geophy. Res. Atmos.* 119. 8137 – 8159.  
796 DOI:10.1002/2014JD021669.

797

798 Levin, Z., Hobbs, P.V., 1971. Splashing of water drops on solid and wetted surfaces:  
799 hydrodynamics and charge separation. *Philosophical Transactions of the Royal Society of*  
800 *London.* 269. 555 – 585. DOI: 10.1098/rsta.1971.0052.

801

802 Li, D., Li, C., Li, J., Yang, W., Xiao, M., Zhang, M., Yang, Y., Yu, K., 2022. Efficient  
803 direction- independent fog harvesting using a corona discharge device with a multi-electrode  
804 structure. *Plasma Sci. Technol.* 24. 1 – 10. DOI: 10.1088/2058-6272/ac6be4.

805

806 Lovett, G.M., 1984. Rates and mechanisms of cloud water deposition to a subalpine balsam  
807 fir forest. *Atmos. Environ.* 18. 361 – 371. DOI: 10.1016/0004-6981(84)90110-0.

808

809 Miller, S.T.K., Keim, B.D., Talbot, R.W., Mao, H., 2003. Sea Breeze: Structure, Forecasting,  
810 and Impacts. *Rev. Geophys.* 41. DOI: 10.1029/2003RG000124.

811

812 Mohan, T.S., Temimi, M., Ajayamohan, R.S., Nelli, N.R., Fonseca, R., Weston, M.,  
813 Valappil, V., 2020. On the Investigation of the Typology of Fog Events in an Arid  
814 Environment and the Link with Climate Patterns. *Amer. Meteor. Soc.* 148. 3181 – 3202.  
815 DOI: 10.1175/MWR-D-20-0073.1.

816

817 Nelli, N., Fissehaye, S., Francis, D., Fonseca, R., Temimi, M., Weston, M., Abida, R.,  
818 Nesterov, O., 2021. Characteristics of Atmospheric Aerosols over the UAE Inferred From  
819 CALIPSO and Sun Photometer Aerosol Optical Depth. *Earth and Space Sci.* 8. 1 – 18. DOI:  
820 10.1029/2020EA001360.

821

822 Nicoll, K.A., Harrison, R.G., Marlton, G., Airey, M., 2020. Consistent dust electrification  
823 from Arabian Gulf sea breezes. *Environ. Res. Lett.* 15. DOI: 10.1088/1748-9326/ab9e20.

824

825 Nicoll, K.A., Harrison, R.G., 2010. Experimental determination of layer cloud edge charging  
826 from cosmic ray ionisation. *Geophys. Res. Lett.* 37. DOI: 10.1029/2010GL043605.

827

828 Nicoll, K.A., 2012. Measurements of Atmospheric Electricity Aloft. *Surv. Geophys.* 33. 991  
829 – 1057. DOI: 10.1007/s10712-012-9188-9.

830

831 Nicoll, K.A., Harrison, R.G., 2016. Stratiform cloud electrification comparison of theory  
832 with multiple in-cloud measurements. *Quart. J. Roy. Meteor. Soc.* 142(700). 2679 – 2691.  
833 DOI: 10.1002/qj.2858.

834

835 Nicoll, K.A., Readle, A., Al Kamali, A., Harrison, R.G., 2022. Surface atmospheric electric  
836 field variability at a desert site. *J. Atmos. Solar-Terr. Phys.* 241. 1 – 11. DOI:  
837 10.1016/j.jastp.2022.105977.

838

839 Nizamuddin, S., Ramanadham, R., 1983. The Electric Potential Gradient in Mist, Haze, and  
840 Fog. *PAGEOPH.* 121. 353 – 359. DOI: 10.1007/BF02590144.

841

842 Roman-Cascon, C., Steeneveld, G.J., Yague, C., Sastre, M., Arrillaga, J.A., Maqueda, G.,  
843 2016. Forecasting radiation fog at climatologically contrasting sites: evaluation of statistical  
844 methods and WRF. *Quart. J. Roy. Meteor. Soc.* 142. 1048 – 1063. DOI: 10.1002/qj.2708.

845 Rycroft, M.J., S. Israelsson and C. Price, 2000: The global atmospheric electric circuit, solar  
846 activity and climate change. *J. Atmos. Solar-Terr. Phys.* 62. 1563 – 1576. DOI:  
847 10.1016/s1364-6826(00)00112-7.

848  
849 Serbu, G.P., Trent, E.M., 1958. A study of the use of atmospheric -electric measurements in  
850 fog forecasting. *Eos Trans. Amer. Geophy. Union.* 39. 1034 – 1042. DOI:  
851 10.1029/TR039i006p01034.

852  
853 Simpson, G.C., 1909. XV. On the electricity of rain and its origin in thunderstorms.  
854 *Philosophical Transactions of the Royal Society of London.* 209. 379 – 413. DOI:  
855 10.1098/rsta.1909.0015.

856  
857 Tag, P.M., 1976. A Numerical Simulation of Warm Fog Dissipation by Electrically  
858 Enhanced Coalescence: Part I. An Applied Electric Field. *J. Applied Meteor. Climatology.*  
859 15. 282 – 291. DOI: 10.1175/1520-0450(1976)015<0282:ANSOWF>2.0.CO;2.

860  
861 Tai, H., Zhuang, Z., Jiang, L., Sun, D., 2017. Visibility Measurement in an Atmospheric  
862 Environment Simulation Chamber. *Current Optics and Photonics.* 1. 186 – 195. DOI:  
863 10.3807/COPP.2017.1.3.186.

864  
865 Tardif, R., Rasmussen, R.M., 2007. Event-Based Climatology and Typology of Fog in the  
866 New York City Region. *J. Applied Meteor. Climatology.* 46. 1141 – 1168. DOI:  
867 10.1175/JAM2516.1.

868  
869 Weston M., Temimi, M., Burger, R., Piketh, S., 2021. A Fog Climatology at Abu Dhabi  
870 International Airport. *J. Applied Meteor. Climatology.* 60. 223 – 236. DOI: 10.1175/JAMC-  
871 D-20-0168.1.

872  
873 Wilson, C.T.R., 1921. III. Investigations on lightning discharges and on the electric field of  
874 thunderstorms. *Philosophical Transactions of the Royal Society of London.* 221. 73 – 115.  
875 DOI: 10.1098/rsta.1921.0003.

876  
877 World Meteorological Organization, 2012. Guide to Meteorological Instruments and  
878 Methods of Observations. Accessed 16 August 2022, from:  
879 [https://library.wmo.int/doc\\_num.php?explnum\\_id=10616](https://library.wmo.int/doc_num.php?explnum_id=10616)

880  
881 Yair, Y., Yaniv, R., 2023. The Effects of Fog on the Atmospheric Electrical Field Close to the  
882 Surface. *J. Atmos.* 14. 1 – 12. DOI: 10.3390/atmos14030549.

883  
884 Zheng, M., Li, J., Li, C., He, F., Li, D., Yu, K., Pan, Y., 2023. Investigation of the effects of  
885 parallel electric field on fog dissipation. *J. Phys. D: Applied Phys.* 56. 1 – 10. DOI:  
886 10.1088/1361-6463/acd85c.

887  
888 Zheng, X.J., 2013. Electrification of wind-blown sand: Recent advances and key issues. *Eur.*  
889 *Phys. J. E.* 36. 1 – 15. DOI: 10.1140/epje/i2013-13138-4.

890  
891 Zhou, L., Tinsley, B.A., 2012. Time dependent charging of layer clouds in the global electric  
892 circuit. *Advances Space Res.* 50. 828 – 842. DOI: 10.1016/j.asr.2011.12.018.

893

894 **Appendix A**

895

896 **A.1 Instrumentation**

897

898

899 **A.1.1 Campbell CS110: Electric Field Meter**

900

901 Being robust to all meteorological conditions makes the electric field mill as one of the reliable  
902 ways for continuous measurements of atmospheric electric fields (Agarwal et al., 2020; Bennett  
903 and Harrison, 2007). The electric field mill consists of a sensing electrode, which is shielded and  
904 exposed via a mechanical shutter (Bateman et al., 2007; Nicoll, 2012). As the electrode vane rotate,  
905 they become shielded and exposed with the aid of the motor, which in turn causes charge to be  
906 induced as it gets exposed (Agarwal et al., 2020; Bennett and Harrison, 2007). This charge is  
907 proportional to the electric field (Harrison, 2015).

908

909 In this research, A Campbell CS110 electric field meter was used to measure the atmospheric  
910 electric fields (see Figure 2(b)). In terms of measurements ranges, the electric field meter was  
911 mounted at 3m above ground and set to measure the electric fields at  $\pm 20$  k V/m. In terms of  
912 datalogging, the electric field data were logged each 1-second, which was then averaged to 1-  
913 minute mean values to conduct this study.

914

915

916

917

918

919 **A.1.2 Biral SWS-100: Visibility Sensor**

920

921 One of the commonly performed meteorological observation is visibility (Tai et al., 2017).  
922 Visibility sensors are considered the main tool in detecting fog. In this study, Biral SWS-100 was  
923 used to estimate the optical range in the site (see Figure 2 (b)). The sensor uses the forward  
924 scattering method to measure the visibility (Izett et al., 2018). This works by sending out a beam  
925 of light from the transmitter, while the receiver measures the light scattered forward by the particles  
926 in the air (WMO, 2012). The visual range decreases as the particles in the air increase, which cause  
927 more scattering of light (Harrison, 2015).

928

929 In this study, the sensor was configured to have a maximum visual range of 50 km and the visibility  
930 data were logged at a time resolution of 1 minute. In addition, the SWS-100 also includes a present  
931 weather sensor, which can help in identifying the presence of fog. One of the issues encountered  
932 was the contamination of the sensor's windows, which was mainly caused due to dust and sand  
933 surrounding the field site.

934

935

936

937

938

939 **A.1.3 Standard Meteorological Sensor**

940

941 To verify the presence of fog and other weather conditions, standard meteorological data were  
942 obtained from an automatic weather station in Al Marmoom, Dubai. As discussed, Al Marmoom  
943 AWS is located about 9 km away from the observation site. This was chosen mainly because no  
944 standard meteorological measurements were available in the observation site until January 2022.  
945 In addition, the station was the closest available to Sanad Academy, in which the results were  
946 expected to link.

947

948 The weather parameters focused on were the wind speed (in m/s) and direction, the RH, and the  
949 dry bulb temperature (in °C). All these parameters were useful in confirming the present weather  
950 in the field site. For example, the wind speed and direction were used to verify some of the sudden  
951 changes in the PG data. In addition, the dry bulb temperature and the RH were used to calculate  
952 the dew point temperature (in °C), which was also useful to confirm the presence of fog. Other  
953 variables such as rainfall amount (in mm), air pressure (in hPa) and solar radiation (in W/m<sup>2</sup>) were  
954 used occasionally for extra support. The standard meteorological data at Al Marmoom AWS were  
955 logged at 15-minute time resolution.

956

957

958

959

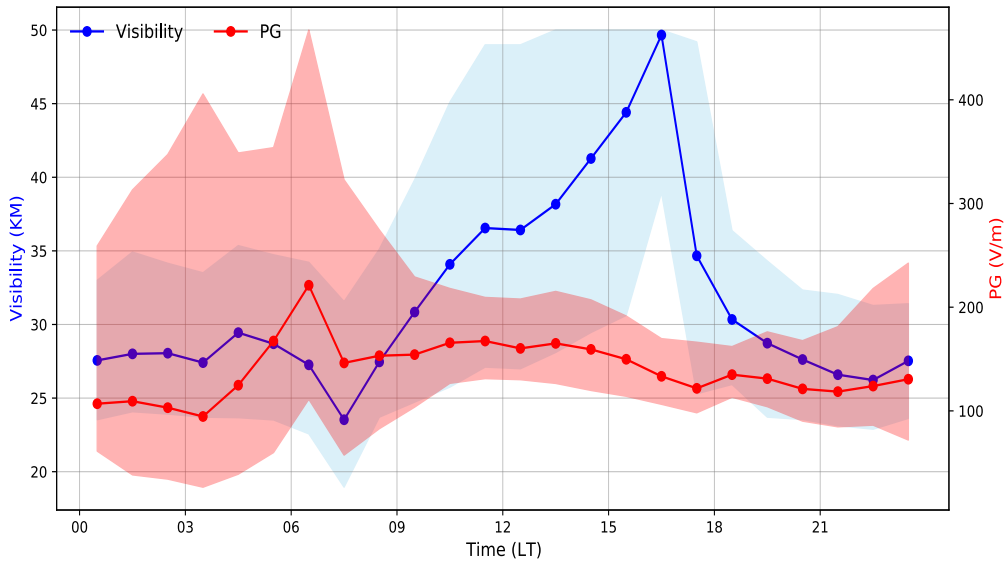
960

961 **A.2 Diurnal variation during fair weather conditions**

962

963 To compare the electrical properties during disturbed weather conditions to those observed during  
964 fair weather conditions, the average typical diurnal variation in PG under fair weather conditions  
965 was derived using data collected throughout the year 2021. The criteria used to identify fair  
966 weather conditions included wind speed less than 4 m/s, visibility greater than 20 km, and present  
967 weather code equals to 0 (i.e., no significant weather observed). A high visibility threshold was  
968 used to minimise the influence of aerosol particles, which can affect the PG measurements. Figure  
969 A1 demonstrates the hourly mean diurnal variation in PG and visibility during fair weather  
970 conditions. The analysis reveals that typical PG values during such conditions are positive with  
971 median values ranging between 90 to 250 V/m, which aligns with the previous findings (i.e.,  
972 Bennett and Harrison, 2007). The peak in PG between 16-17LT is likely to be associated with the  
973 arrival of the sea breeze front (e.g., as observed for other UAE sites (Nicoll et al, 2022)). When  
974 compared to the foggy events, the PG during fair weather conditions demonstrates lower  
975 variability with fewer sharp changes, and exclusively positive PG values.

976



978 Figure A1. Diurnal variation in PG and Visibility along with the interquartile ranges under fair  
 979 weather conditions at Sanad Academy. The displayed data points are hourly medians using 1-  
 980 minute values throughout all 2021 data. The criteria used to identify fair weather conditions  
 981 included wind speed less than 4 m/s, visibility greater than 20 km and present weather code equals  
 982 to 0 (i.e., no significant weather).